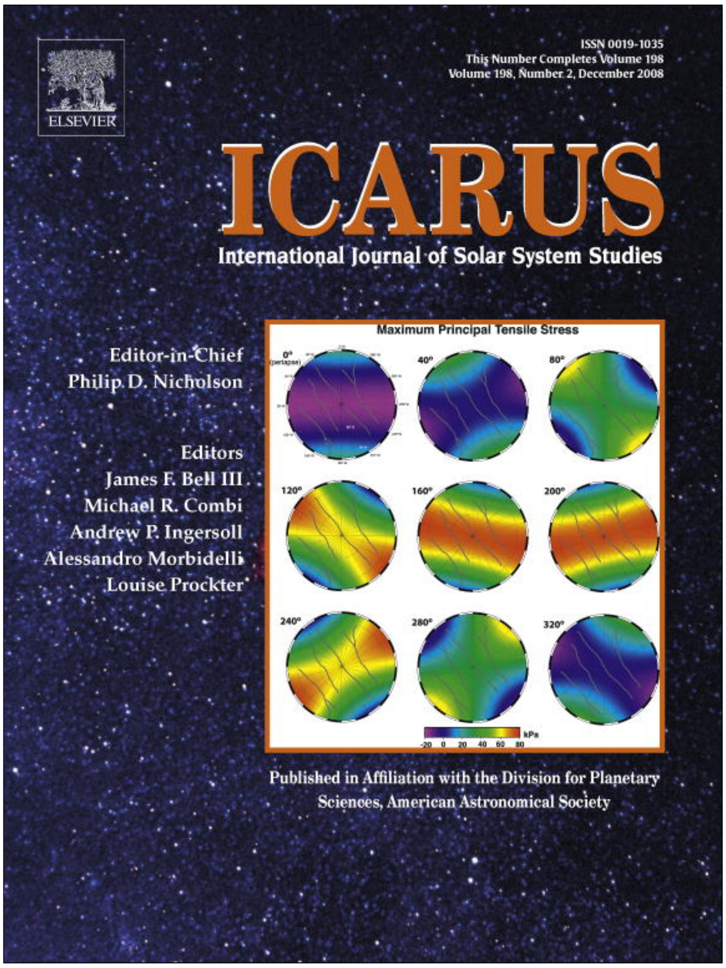
ELSEVIER
ISSN 0019-1035
This Number Completes Volume 198
Volume 198, Number 2, December 2008
ICARUS
International Journal of Solar System Studies
Editor-in-Chief
Philip D. Nicholson
Editors
James F. Bell III
Michael R. Combi
Andrew P. Ingersoll
Alessandro Morbidelli
Louise Prockter
Maximum Principal Tensile Stress
Published in Affiliation with the Division for Planetary Sciences, American Astronomical Society

Icarus 198 (2008) 351–364

Contents lists available at ScienceDirect

Icarus

www.elsevier.com/locate/icarus

Evidence for ponding and catastrophic floods in central Valles Marineris, Mars

Keith P. Harrison [a,*], Mary G. Chapman [b]

[a] Southwest Research Institute, 1050 Walnut Street, Ste 300, Boulder, CO 80302, USA
[b] US Geological Survey, 2255 N. Gemini Drive, Flagstaff, AZ 86001, USA

ARTICLE INFO

Article history:
Received 26 March 2008
Revised 4 August 2008
Available online 4 September 2008

Keywords:
Mars
Mars, surface

ABSTRACT

The Valles Marineris canyon system of Mars is closely related to large flood channels, some of which emerge full born from chaotic terrain in canyon floors. Coprates Chasma, one of the largest Valles Marineris canyons, is connected at its west end to Melas Chasma and on its east end to chaotic terrain-filled Capri and Eos Chasmata. The area from central Melas to Eos Chasmata contains a 1500 km long and about 1 km deep depression in its floor. Despite the large volumes of groundwater that likely discharged from chaotic terrain in this depression, no evidence of related fluvial activity has thus far been reported. We present an analysis of the regional topography which, together with photogeologic interpretation of available imagery, suggests that ponding due to late Hesperian discharge of water possibly produced a lake (mean depth 842 m) spanning parts of the Valles Marineris depression (VMD). Overflow of this lake at its eastern end resulted in delivery of water to downstream chaos regions and outflow channels. Our ponding hypothesis is motivated primarily by the identification of scarp and terrace features which, despite a lateral spread of about 1500 km, have similar elevations. Furthermore, these elevations correspond to the maximum ponding elevation of the region (−3560 m). Simulated ponding in the VMD yields an overflow point at its eastern extremity, in Eos Chasma. The neighborhood of this overflow point contains clear indicators of fluvial erosion in a consistent east–west orientation.

1. Introduction

The circum-Chryse outflow channels have trough (chasma) and chaos sources, and appear to have formed in the Late Hesperian to Early Amazonian (Scott and Tanaka, 1986; Chapman and Scott, 1989; Witbeck et al., 1991; Rotto and Tanaka, 1995). In particular, Tiu and Simud Valles can be traced both to chaotic terrains and to the opened, connected eastern ends of Capri, Eos, Coprates, and Melas Chasmata. These four chasmata are part of a system of troughs that compose the Valles Marineris on Mars—the largest array of interconnected canyons in the Solar System, over 3200 km in length. The Valles Marineris chasmata have been generally interpreted as large grabens and collapse structures, produced in association with tensional stresses generated by the Tharsis rise during the Late Noachian to Early Hesperian (Scott and Tanaka, 1986; Witbeck et al., 1991; Lucchitta et al., 1992). Dynamic upwarping and rising magma caused by a local mantle plume may account for structures at Tharsis (Hartmann, 1973; Carr, 1974; Wise et al., 1979). Chaotic terrains at channel sources consist of jumbled and subsided blocks of material that may be explained by collapse of overlying rocks due to ground ice melting and expulsion of groundwater and rock debris (Sharp, 1973; Saunders, 1979; Komatsu et al., 2000). Magmatic intrusion may have provided the energy for melting (Masursky et al., 1977; Max and Clifford, 2000). Elevation data from Viking and from the Mars Global Surveyor (MGS) Mars Orbiter Laser Altimeter (MOLA) show that, like the chasmata, most chaotic terrains also lie in topographic depressions. Any groundwater discharged to the surface after the formation of these depressions must have ponded locally: the only available outlets are channel head regions that generally lie above the depression floors (e.g. Coleman et al., 2007). Ponding depths required to access circum-Chryse channel heads are substantial, ranging from 100s to 1000s m (Harrison and Grimm, 2008). As suggested by Chapman and Tanaka (2002), the presence of the outflow channels themselves also suggests ponding: catastrophic terrestrial floods usually form due to failure of natural or man-made dams. Such is certainly the case for the Channeled Scablands of Washington State (Bretz et al., 1956), although the original source of dammed water for these channels was meltwater from large Pleistocene ice sheets, not groundwater discharge at chaotic terrains. In Valles Marineris, from central Melas to Eos Chasmata, MOLA topography indicates a net uphill gradient of 0.03° across 1500 km. Assuming that this gradient has not been modified by later tectonism or resurfacing, it would have resulted in a 1-km-high barrier to water flowing out to the Chryse channels (Smith et al., 1999). This central Melas to Eos Chasmata topographic low is 1500 km wide and for the rest of this paper, will be referred to as the Valles Marineris depression or VMD. We em-

* Corresponding author.
E-mail address: harrison@boulder.swri.edu (K.P. Harrison).

0019-1035/$ – see front matter
doi:10.1016/j.icarus.2008.08.003

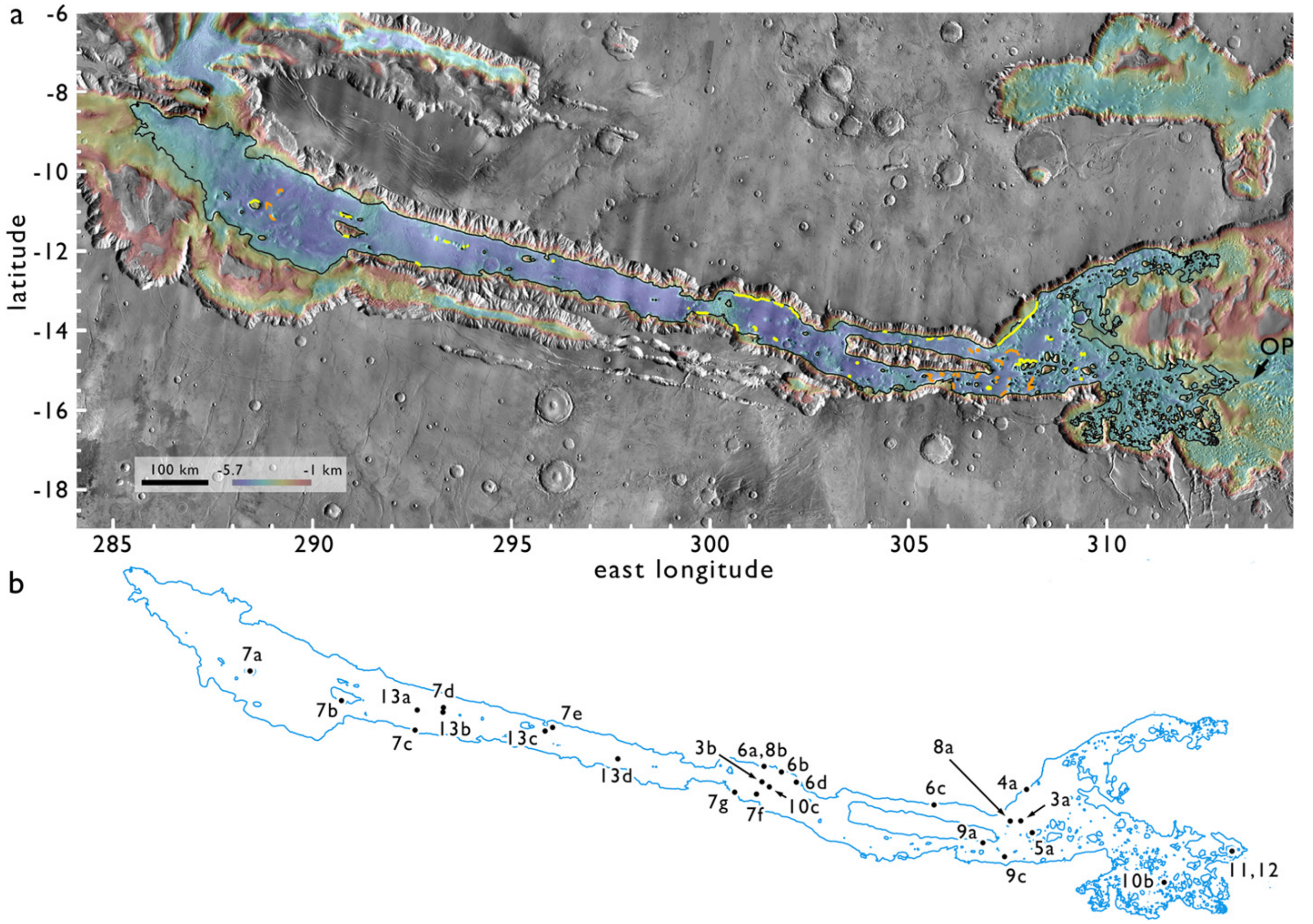

Fig. 1. (a) Location of putative paleolake in the central Valles Marineris. Black contour defines the maximum ponding elevation, with overflow point indicated by "OP." Yellow and orange marks indicate possible lacustrine features described in the text as bench types *I* and *II* respectively. The underlying image is a THEMIS daytime IR mosaic with gridded MOLA data at elevations below −1 km shown in color. (b) The maximum ponding level contour provides context for other figures in this work. Dots correspond to the centers of figure images.

phasize that this depression occupies, on average, only the lowest few hundred m of the central Valles Marineris canyons.

Although source depressions and catastrophic channels are suggestive of ponding, they do not constitute direct evidence thereof. Instead, evidence takes the form of shoreline and other morphologies found (thus far) in four depressions associated with the circum-Chryse outflow channels: Hydraotes Chaos (Ori and Mosangini, 1998), Aram Chaos (Glotch and Christensen, 2005), Shalbatana Vallis (Di Achille et al., 2007), and Juventae Chasma (Coleman and Baker, 2007). Gorgonum Chaos, a chaotic terrain west of the Tharsis rise, may also have held standing bodies of water (Howard and Moore, 2004).

The geologic history of the Valles Marineris is complex, involving fluvial (Mangold et al., 2004), tectonic (Schultz, 1991; Peulvast et al., 2001; Mège et al., 2003), volcanic and eolian (Lucchitta et al., 1994; Chapman and Tanaka, 2002), mass-wasting (Lucchitta, 1979), and collapse processes (Tanaka and Golombek, 1989). In addition to these mechanisms, lacustrine activity has also been inferred, usually from characteristics of the large interior layered deposits on canyon floors (Komatsu et al., 1993; Lucchitta et al., 1994; Greeley et al., 2003). Coleman et al. (2007) used channel elevations to infer ponding in eastern Capri Chasma (northeast of the VMD) during the early stages of circum-Chryse outflow channel formation. We provide possible evidence for a paleolake that may have filled the VMD itself. Shorelines and other features indicate formation near the end of outflow channel activity (late Hesperian) due to groundwater discharge, with subsequent release of water into the Tiu and Simud outflow channels. Limited ponding episodes may have extended into the early Amazonian.

2. Methods

The inundated area of the VMD (Fig. 1) was generated using an iterative algorithm that takes as its input gridded MOLA elevation data at 128 pixels/degree resolution. At each iteration, the algorithm considers an inundation area containing all points whose elevation falls below a lake surface elevation incrementally higher than that of the previous iteration. It then removes those points not in contiguous contact with a predetermined source location (in this case, the deepest part of the Capri Chasma chaotic terrain, a reasonable source of discharged groundwater for VMD ponding). Our first iteration used an arbitrarily low initial lake surface elevation, yielding a small inundated area. The incremental increase in lake elevation with successive iterations caused the inundated area to expand, and the algorithm was halted just before chaos and channel regions outside the VMD were inundated. The lake surface elevation (−3560 m) used for the last iteration was taken as the maximum ponding elevation of the VMD. Conclusive evidence of shoreline formation above this elevation is lacking, suggesting that shorelines were emplaced after the last significant overflow event, or that episodic dam failure limited the duration of ponding

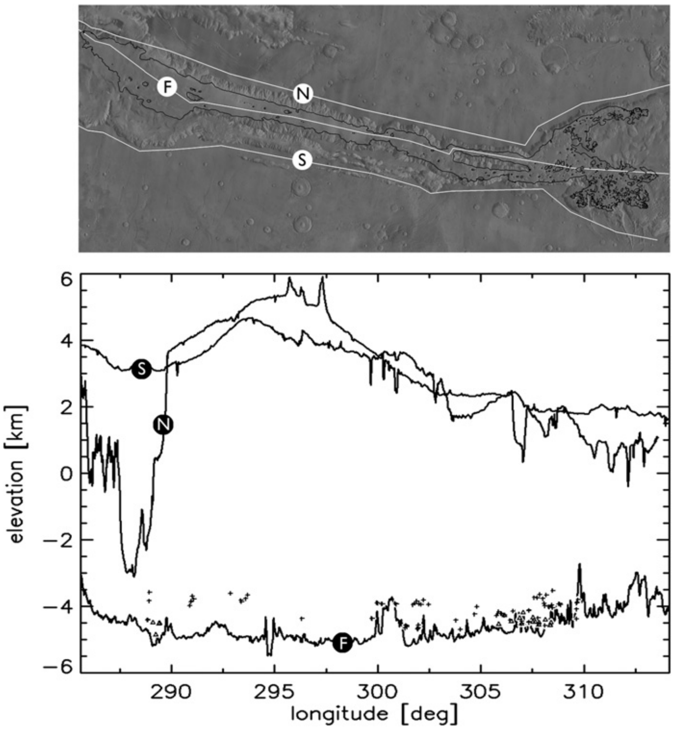

Fig. 2. Elevation profiles along the floor ("F") of the putative paleolake in the VMD and along plateau surfaces immediately to the north ("N") and ("S"). In the lower panel, plus signs mark individual MOLA shot elevations of bench features marked in yellow and orange in Fig. 1. The upper panel is a THEMIS daytime mosaic.

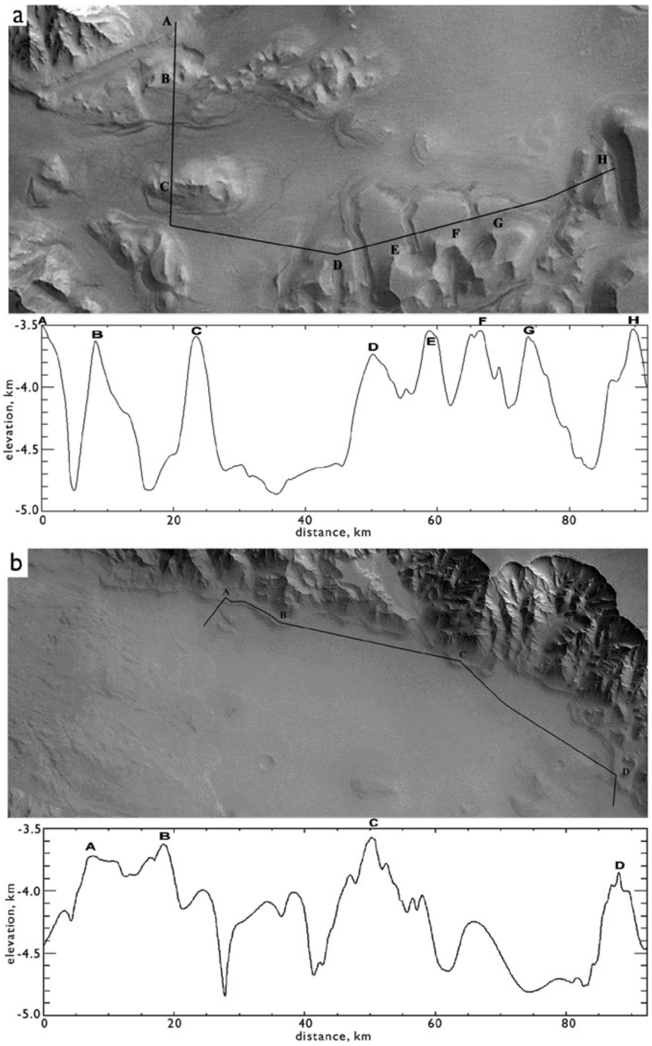

Fig. 3. HRSC images and topographic profiles: (a) north wall to center of west Capri Chasma, image (from orbit 0394_0009) is merged with topography; (b) north wall of east Coprates Chasma (orbit 0438_0000). Letters indicate points at which the profiles cross bench landforms. Note the similar elevations of these points.

at higher levels to the extent that significant shoreline formation was not possible. Note that the overflow level is significantly lower than canyon rim elevations (Fig. 2) and yields an average ponding depth of 842 m, small compared to the canyon depth of 5 to 10 km. Nonetheless, the maximum volume of water the lake could have held is 110,000 km^3, similar to that of the large paleolake proposed for the Ma'adim Vallis drainage basin (Irwin et al., 2002). Another important result from our inundation algorithm is that overflow from the VMD would first occur in Eos Chasma at a location (Fig. 1) associated with fluvial features described in greater detail in Section 3.3.

3. Morphological features

Within the VMD, we can now detect two distinct levels of low topographic benches observable on recent high-resolution data sets from the MGS Mars Orbital Camera (MOC), the Mars Odyssey Thermal Emission Imaging System (THEMIS), HRSC, and the Mars Reconnaissance Orbiter CTX and HiRISE instruments. The bench deposits, and a dichotomy in central massif characteristics, occur close to the maximum putative lake level of the VMD. In addition, the topographically-derived overflow point of the VMD coincides with erosive fluvial features, providing a strong argument for ponding. We proceed with a detailed description of bench, massif dichotomy, and overflow morphologies, followed by a description of the VMD floor.

3.1. Bench morphology

We present two groups of features that may be associated with shoreline processes. The first consists of benches distributed across the VMD at two distinct topographic levels. The second consists of a morphological dichotomy on the slopes of massifs interior to the putative paleolake boundary. We consider bench morphology first. An upper, more prominent bench (which we denote with the roman numeral *I*) ranges in height from a few 100 m to over 1 km above the adjacent depression floor, while a more local, and less distinct bench (*II*) is observed at lower elevations. A key collective property of the observed benches is that they both lie within (and for bench *I*, close to) the area that would be inundated by a lake filled to the maximum ponding level of the region (−3560 m).

3.1.1. Bench I

This topographically higher bench is locally observed along the north and south walls of the VMD and around massifs and chaotic blocks on the floor of the chasmata (yellow marks in Fig. 1). This bench locally forms a basal terrace beneath the easily recognizable cliffs and spur-and-gully outcrops of wallrock around the VMD, and on wallrock inselbergs within the VMD, and is not observable outside the depression area. A relatively flat esplanade of resistant surface material overlain by talus materials separates the top of bench *I* from the adjacent proper wallrock outcrops above it. Bench morphology is similar to that observed elsewhere on Mars, including nearby Hydraotes Chaos (Ori and Mosangini, 1998) and Shalbatana Vallis (Di Achille et al., 2007). Bench widths vary from 10s m to 10s km, and heights vary from a few 100 m to about 1500 m relative to the adjacent depression floor (Figs. 2 and 3). In some cases, multiple benches occur at different elevations lo-

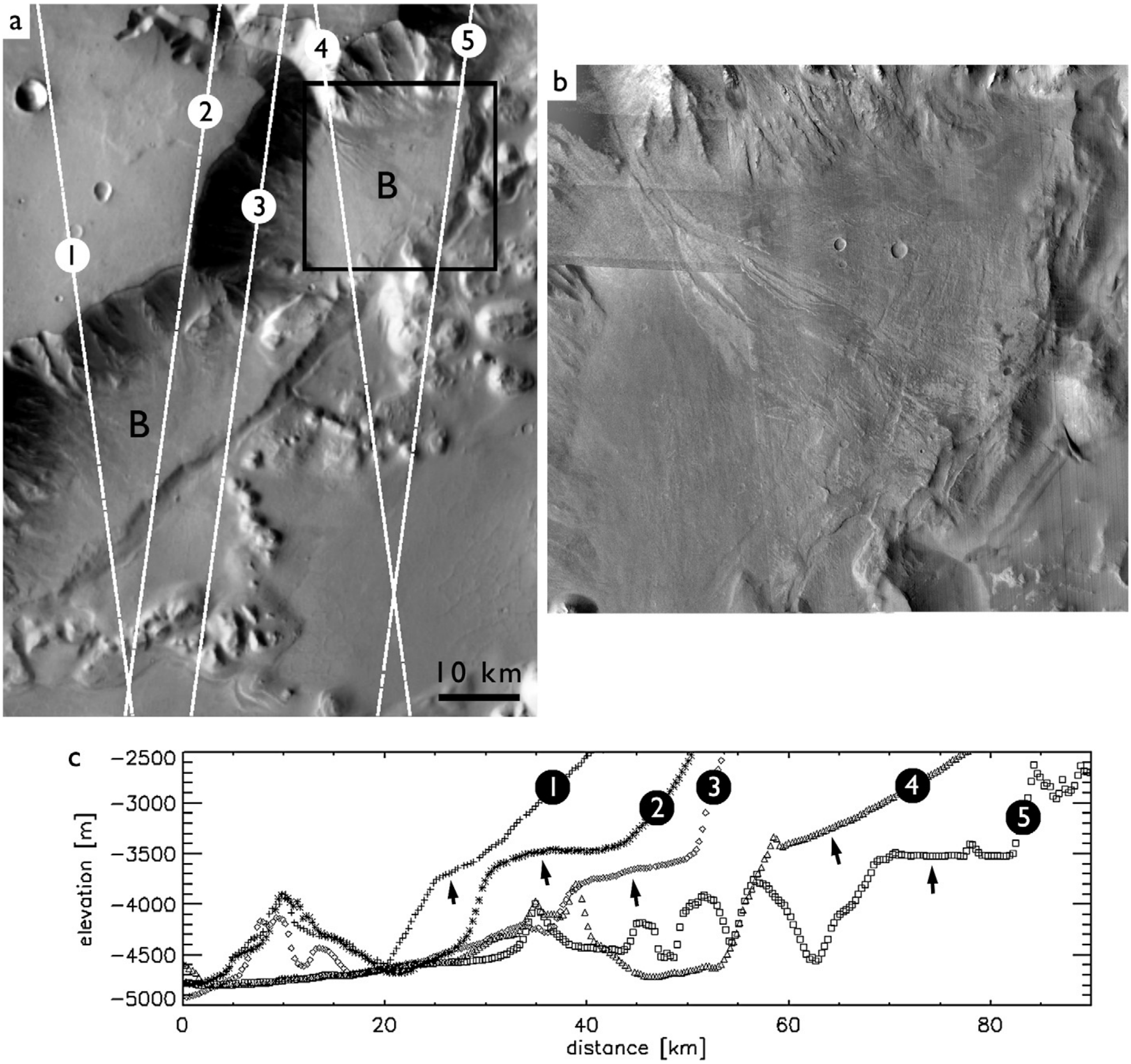

Fig. 4. (a) Bench ("B") along SE-facing wall of Capri Chasma (THEMIS daytime mosaic). (b) A network of divergent valleys exits a tributary canyon in the Capri Chasma wall and traverses a fan-shaped mound on the bench (see black box in (a) for context; THEMIS VIS V06344002 and V16865001). (c) Elevation profiles of numbered MOLA tracks in (a). Arrows indicate bench location. Track 4 covers the length of the alluvial fan in (b). Track 5 demonstrates the uniform elevation of the bench front close to the maximum ponding elevation of the region (−3560 m).

cally. Benches are generally arcuate in planform, with surfaces that are level to concave. They have a smoother texture than the scarps they abut and appear to be layered. The benches are concentrated in east Coprates Chasma and Capri Chasma, where they are also most pristine. Canyon walls are considerably higher in the western part of the VMD (Fig. 2), suggesting that mass wasting has degraded the lower walls and floor to a greater extent here.

Locally, the widest section of bench *I* skirts the SE-facing wall of Capri Chasma (Fig. 4a). Talus deposits and an apparent alluvial fan (Fig. 4b) cover much of the bench, yielding a gentle slope toward the canyon interior. However, where the bench is unaffected by these structures, it is remarkably level (Fig. 4c). A MOLA track along the bench front (track 5, Fig. 4c) demonstrates a uniform absolute elevation of −3510 m.

Further south in Capri Chasma is a set of benches along the northern edge of a massif in the chasma floor (Fig. 5). Again, the elevation of the benches is quite uniform. The benches are separated by narrow re-entrants that appear to be related to amphitheater-shaped source regions cut into the central massif. The re-entrants are likely fluvial sapping features enlarged by wind erosion and which postdate bench formation. A groundwater sapping interpretation is in line with similarly interpreted features elsewhere in the Valles Marineris (e.g. Echus, Juventae, and Ius Chasmata; Harrison and Grimm, 2005). Other processes such as mass-wasting and fluvial processes cannot, however, be ruled out.

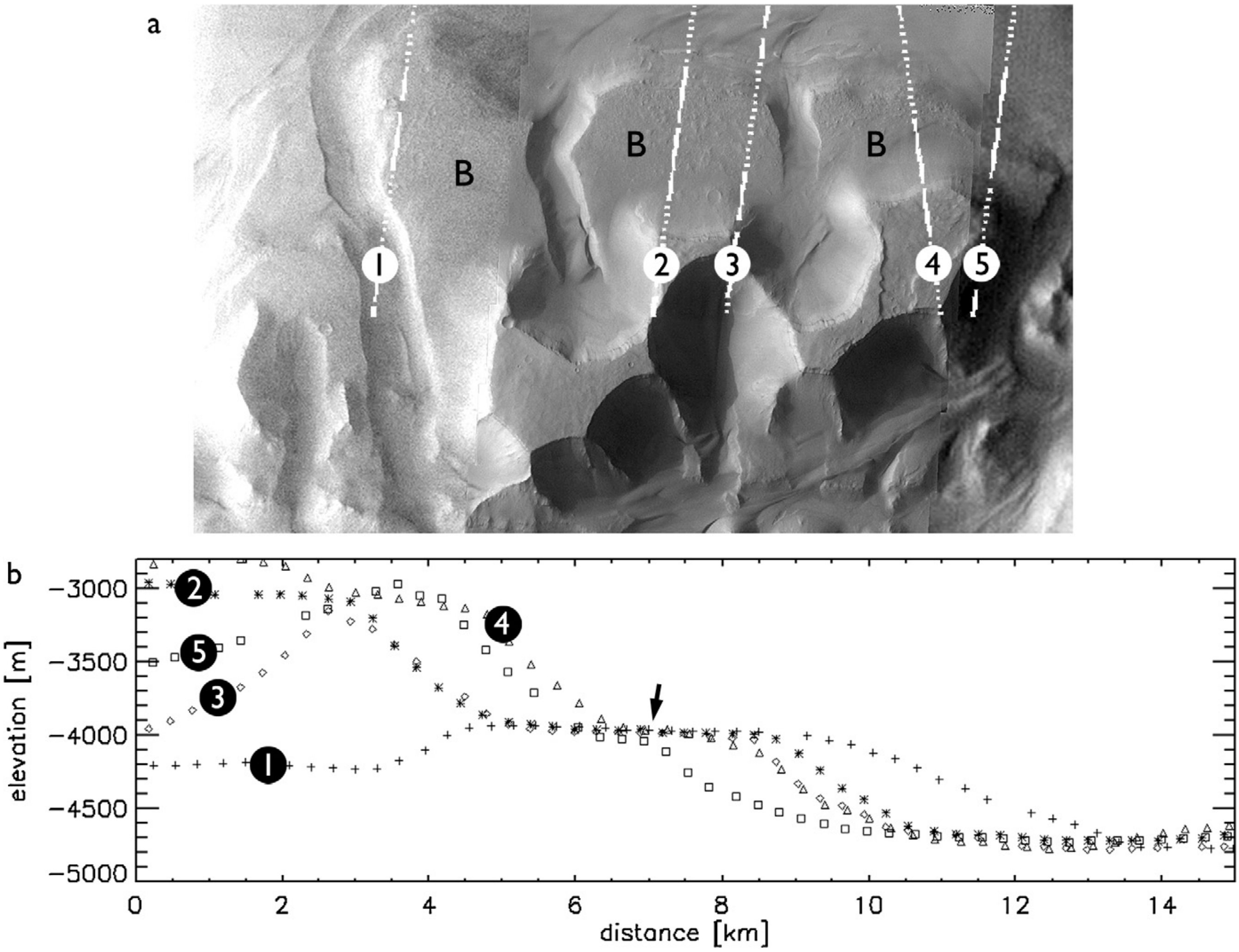

Fig. 5. (a) Benches ("B") along the north-facing scarps of mesas in Capri Chasma (THEMIS VIS and daytime IR mosaic). Narrow reentrants between benches appear to be related to amphitheater-shaped source regions cut into the mesas. (b) Elevation profiles of numbered MOLA tracks in (a). Arrow indicates bench location.

The parallel arrangement of the re-entrants suggests preferential formation along faults.

Further examples of bench *I* in the VMD are shown in Figs. 3b, 6, and 7. The outcrops of benches in Fig. 6 occupy a 500 km stretch of the north wall of Coprates Chasma, while those in Fig. 7 are further west in Melas and western Coprates Chasmata. Images of bench *I* taken by the Mars Reconnaissance Orbiter Context (CTX) Camera show horizontal layering within the upper caprock of the bench (Fig. 8a). These layers follow the same trend as layers within the resistant cliffs and also spur-and-gully outcrops of surrounding Valles Marineris wallrock. Points and re-entrants in the bench are mimicked by overlying layers in the wallrock proper (Fig. 8b). Although a constructionally formed bench might be expected to duplicate the pre-existing trends of the Valles Marineris wallrock to some degree, the observed relations suggest that bench *I* may instead be a low level of layered wall rock separated from wallrock proper by less resistant materials that tend to form talus deposits. Local benches with multiple elevations likely represent the cropping out of separate underlying layers within this bench. Consequently, bench *I* elevations are not expected to conform to a single value. Nonetheless, with a standard deviation of 310 m (around a mean of −4100 m), bench *I* elevations (Fig. 2) are remarkably similar, especially considering their E–W spread of 1280 km. Indeed, this standard deviation is smaller than the corresponding values of 1700 and 560 m for the Clifford and Parker (2001) Contact 1 and 2 shorelines, although these contacts have considerably greater length and may have been affected by polar wander (Perron et al., 2007). The standard deviation is also smaller than those of the north and south plateaus adjacent to the VMD, which are 1850 and 1220 m respectively (using the traces of Fig. 2). Finally, shoreline elevations vary less than paleolake floor elevations: the standard deviation of all gridded MOLA data falling within the maximum ponding level is 450 m. We note, however, that sediment settling from a VMD paleolake would likely have smoothed the VMD floor to some degree. The lake hypothesis therefore eschews large standard deviations in floor elevation, and the moderate value of 450 m supports this view.

3.1.2. Bench II

This bench level (orange marks in Fig. 1) lies below bench *I* and therefore also below the maximum putative lake level of the VMD. Mean elevation is -4500 ± 140 m. Bench *II* has a soft sinuous scarp edge where it surrounds blocks of material and islands of wallrock within the VMD (Figs. 9a and 9c). The bench has an approximate maximum height of only 200 m, and is frequently too small to be resolved properly by MOLA or HRSC topography. Layering is not observed within this bench. In many areas, the bench is overlapped by eolian dunes (Fig. 9c). Bench *II* is observed in Melas Chasma and again in Capri and eastern Coprates

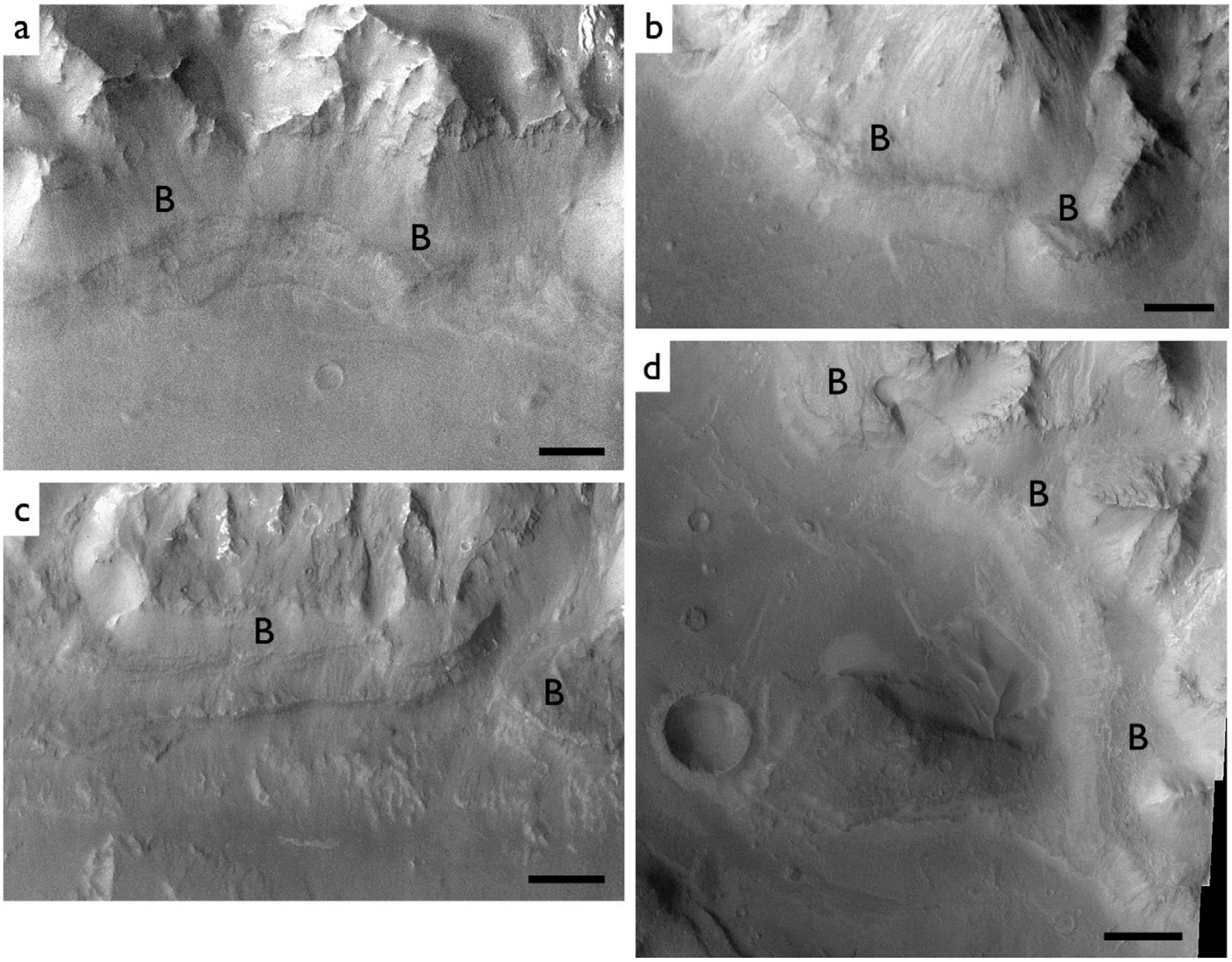

Fig. 6. Examples of bench *I* morphology along the north wall of eastern Coprates Chasma (see Fig. 1 for context). "B" marks the bench in each case. Scale bar in each panel represents 2 km. (THEMIS VIS: (a) V15168001, (b) V16079001, (c) V16915001, (d) V16990002.)

Chasmata, and is separated from bench *I* by another broad low esplanade. Locally bench *II* has marginal fractures suggesting collapse of the bench front (Figs. 9a and 9c). Similar fissures have been observed along Gorgonum Chaos benches (Fig. 9b; Howard and Moore, 2004) and around knobs in the northern plains (Tanaka, 1997; Tanaka et al., 2003). While the Gorgonum Chaos fissures are only ∼10 m across, compared to the ∼250 m of the Coprates and Capri features, their similar morphologies may suggest that, like in Gorgonum Chaos, rotation and collapse of the bench *II* margin occurred in response to lowering of the neighboring floor.

3.2. *Massif morphology*

A survey of massifs in the VMD suggests a dichotomy in peak morphology. We surveyed all massifs covered by THEMIS VIS images, including blocks of chaotic terrain in Eos and Capri Chasmata and more isolated massifs in Melas and Coprates Chasmata. Each massif was rated on a continuous qualitatively-based scale from 0 to 1, with 0 corresponding to flat-topped or mesa-like morphology and 1 corresponding to sharply peaked, rugged morphology. The results, grouped into 11 bins (Fig. 10), show that massifs with peaks above the maximum ponding elevation of the VMD are predominantly sharply peaked, usually with spur-and-gully formations typical of canyon wall morphology. The small number of mesa-like morphologies in this group appear to be limited to chaotic blocks which preserve the level topography of the original plateau from which they were broken. Massifs with peaks below the maximum ponding level are more varied but are skewed toward flatter morphologies. Low massifs with peaked morphologies seldom exhibit rugged spurs and gullies but consist more commonly of simple ridges grading smoothly into the canyon floor. A χ^2 test indicates that the probability of the sub- and super-ponding level populations being the same is less than 10^{-4}, confirming that the observed dichotomy is statistically significant.

We note also that a dichotomy in massif scarp morphology was observed, with tall massifs exhibiting spur-and-gully morphology along the upper parts of their walls, with a smoother apron below (e.g., Fig. 10b). This dichotomy is likely due to the formation of talus deposits, but its consistent appearance at the maximum ponding level of the VMD region, and its often sharp delineation, may suggest erosion through shoreline and/or channel flow processes.

3.3. *Possible lacustrine ponding and overflow*

Bench *I* elevations occupy a range abutting the maximum ponding level of the VMD, and bench morphology is flat relative

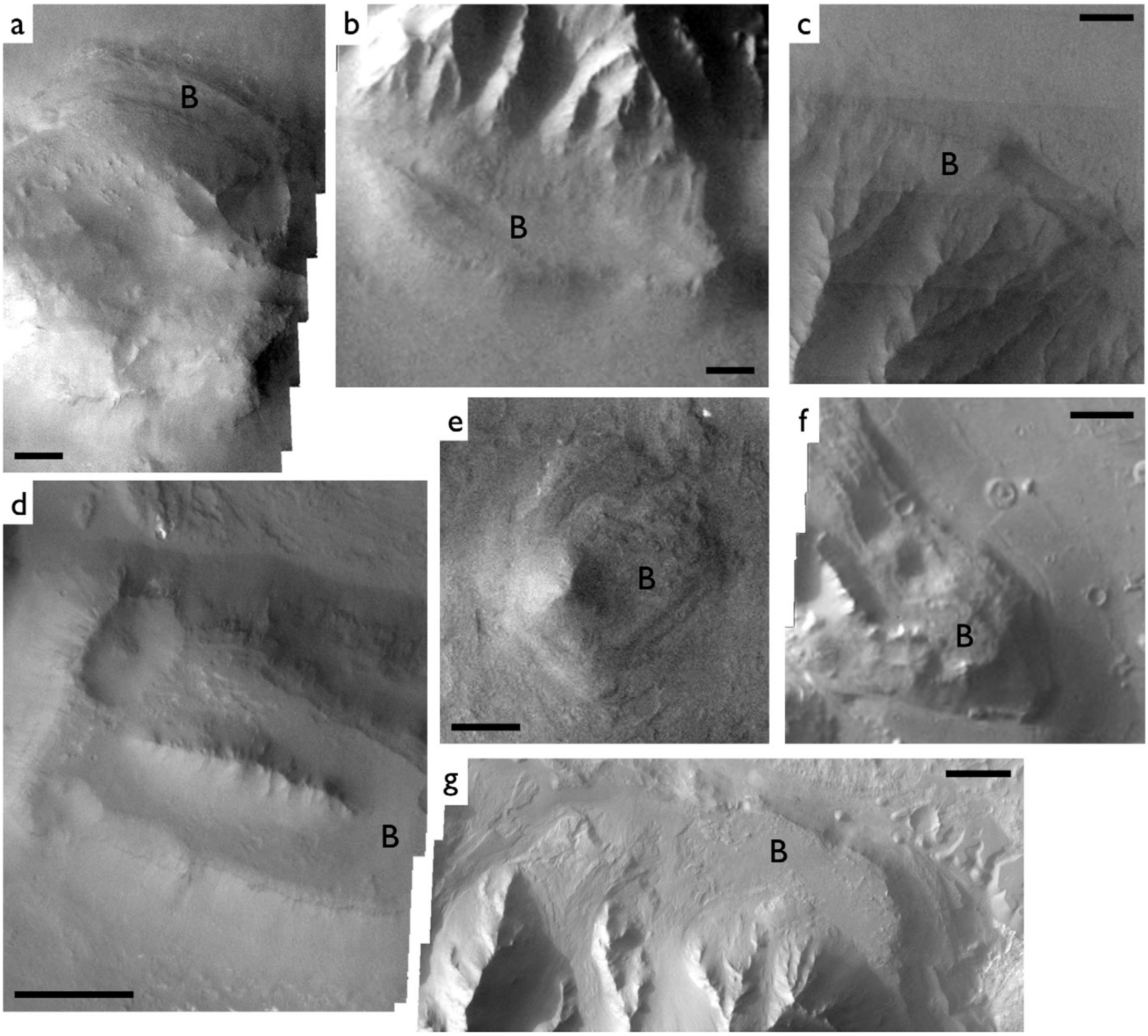

Fig. 7. Examples of bench *I* morphology in eastern Melas and western Coprates Chasmata. "B" marks the bench in each case. Scale bar in each panel represents 2 km. (THEMIS VIS: (a) V15755002, (b) V05683002, (c) V14432002, (d) V16878002, (e) V14357002, (f) V04659002, (g) V18862002.)

to neighboring wallrock. We are thus led to suggest that the bench enclosed a putative paleolake that enhanced the erosional face of the cliffs. On the other hand, the sinuous, locally collapsed edge of bench *II*, together with its lack of layering, suggests that this bench is not part of the Valles Marineris wallrock and is instead morphologically analogous to terrestrial lacustrine terraces. Thus, while the two bench types likely formed under different conditions, they both appear to have been influenced by ponded water in the VMD.

Perhaps the strongest evidence for VMD ponding is the coincidence of the MOLA-derived overflow point in Eos Chasma with a set of scour and channel features (Figs. 11 and 12). Carr (1996) noted that these "sculpted, streamlined" forms could be attributed to catastrophic release of ponded water in an easterly direction, a view supported more recently by Greeley et al. (2003). Large-scale fluvial features within the maximum ponding contour appear to be limited to the overflow region. The orientation of the features suggests a convergence of flow from a relatively wide area in the west toward a narrow eastward exit point. Features appear to be predominantly erosive, suggesting an energetic flow and are analogous in appearance to terrestrial catastrophic flood bars. MOLA profiles near the overflow point suggest a channel depth of about 100 m, implying that prior lake levels could have exceeded the nominal −3560 m ponding level by at least this amount. We note that the general lack of well-defined bench forms above the ponding level suggests that higher lake levels attained over the history of VMD ponding were either too short lived for benches to form or that freezing inhibited shoreline development. Alternatively, the observed shorelines were formed after the last overflow episode.

The apparent flow path downstream of the overflow point leads directly to the channel connecting Eos Chasma with the next large chaotic terrain, Aurorae Chaos. Although Aurorae has lower elevations than the surrounding unbroken plateaus, its floor does not form a regional depression, and flow entering it from Eos Chasma would continue northward to Hydraotes Chaos. The floor of Hy-

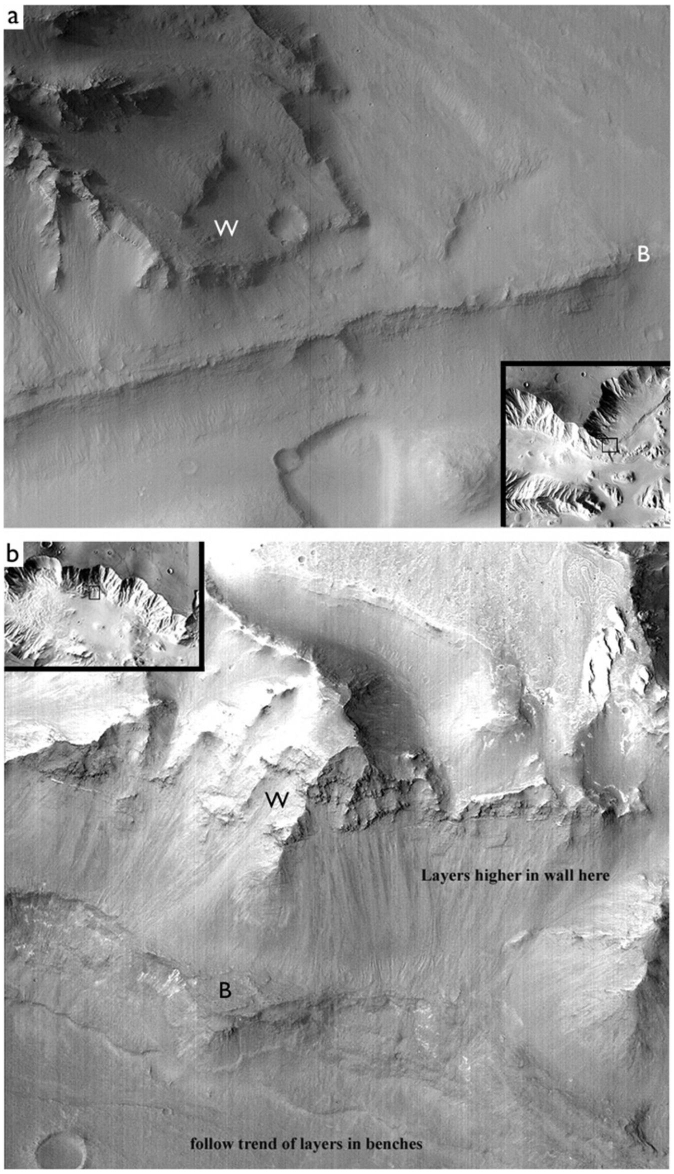

Fig. 8. Horizontal layering in wallrock ("W") and nearby bench *I* morphology ("B"); (a) north wall of west Capri Chasma (P03_002115_1651_XN_14S052W); (b) north wall of east Coprates Chasma (P07_003869_1655_XN_14S058W).

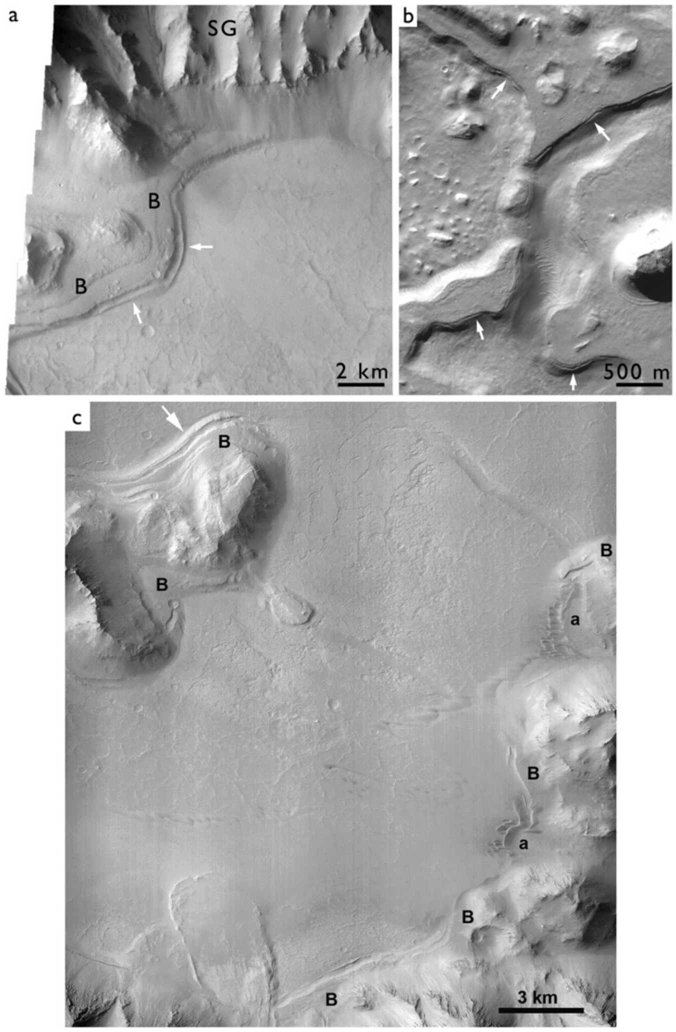

Fig. 9. Examples of bench *II* morphology. (a) A low bench ("B") in east Coprates Chasma (THEMIS VIS V18113004); (b) benches in Gorgonum Chaos, for comparison (MOC M2101910; Howard and Moore, 2004); (c) low benches ("B") in southeast Coprates Chasma ("a" denotes overlying aeolian dunes; CTX image P03_002115_1651_XN_14S052W). White arrows in each frame indicate fractures.

draotes does form a depression, and the likelihood of ponding here is supported by benches encircling chaos blocks (Ori and Mosangini, 1998). Bench morphology is similar to that observed in Capri and Eos Chasmata. Continued northward flow from Hydraotes Chaos would produce some shallow ponding in Simud Valles and then continue to the northern plains. Thus, only two of the large chaos regions linking Coprates Chasma to the northern plains are capable of ponding water to significant depths, and the same two regions (and no others along this flow route) are found to exhibit benches along massif and/or canyon walls. The action of lacustrine processes may have strongly influenced this relationship.

The VMD overflow point is connected to the Aurorae Chaos entrance by a smooth deposit designated by Witbeck et al. (1991) as chasma channel material which includes "material transported and deposited by flowing water." Flow downstream of the VMD overflow point likely spread laterally in this region and deposited some of its sediment load before continuing on to Aurorae Chaos.

3.4. Floor morphology

On a regional scale, the VMD floor is flat relative to the neighboring canyon plateaus (Fig. 2), suggesting that it has been substantially modified since its original formation as a graben. Alternatively, regional changes in plateau elevation following graben formation were not imparted to the canyon floor. However, the abundance of processes able to modify the floor, including mass wasting and chaotic terrain processes, support the former hypothesis.

Lacustrine activity may have contributed to the current floor morphology. A pattern of polygonally arranged ridges is found on the floor of eastern Coprates adjacent to the bench of Fig. 9a, and to the east and north in the lowest parts of the Capri Chasma floor (Fig. 13). Ridge morphology appears to resemble that of Hesperian volcanic plains wrinkle ridges, but an order of magnitude more closely spaced (few km vs few 10s km). MOLA tracks crossing the Capri Chasma ridges do suggest, in some cases, an offset in elevation on either side of each ridge as expected for movement along thrust faults, the widely accepted mechanism behind wrinkle ridge formation. Possibly, the dessication of a volatile-rich floor deposit caused the floor to sink, with resulting compressional forces leading to polygonally arranged thrust faults in the rigid desiccated

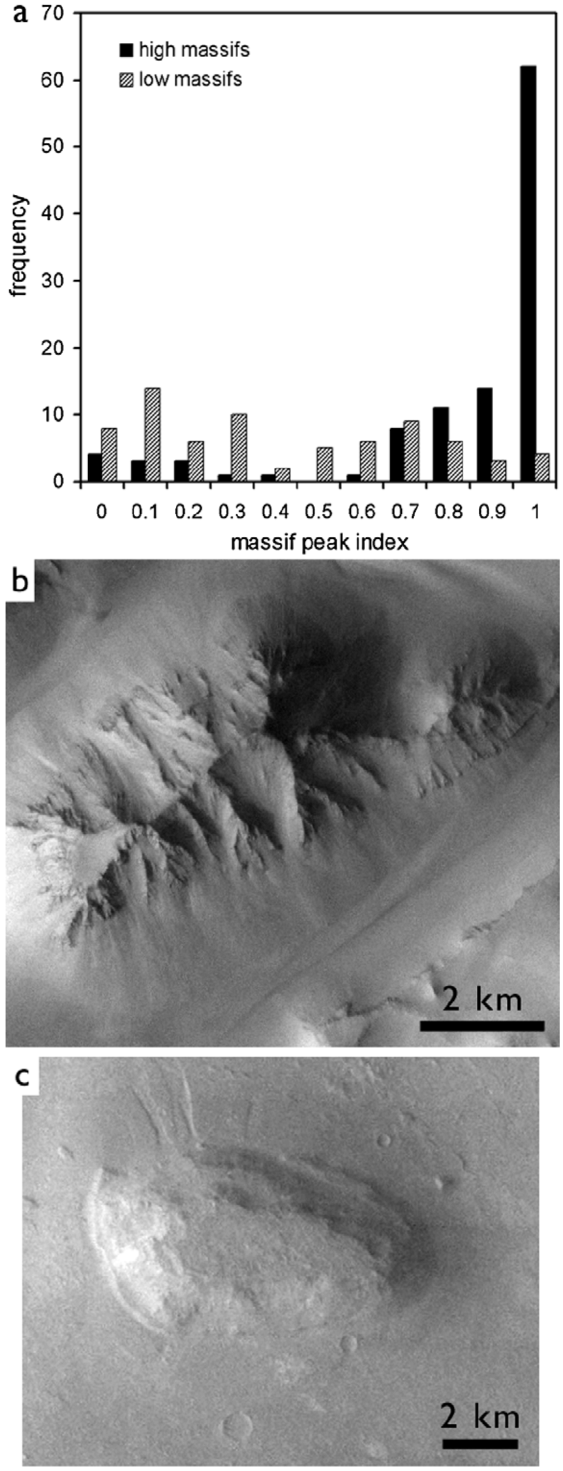

Fig. 10. (a) Morphology of massif peaks in the VMD expressed as a qualitative index ranging from 0 for flat-topped peak morphologies to 1 for sharply crested, rugged peak morphologies. "Low massifs" are those with peak elevations below the maximum ponding level of the VMD; "high massifs" have peaks above this level. High massifs are predominantly sharply crested as indicated by a massif with an index of 1 in (b), while low massifs, although more varied, are skewed toward the flatter morphologies, as indicated by a massif with index 0 in (c). ((b) THEMIS VIS V16478004, (c) V06881001.)

cap at the surface of the deposit. Ridges are found in large, smooth areas of the canyon floor devoid of chaotic blocks that might otherwise have interrupted the lowering and compression process. The marginal fractures on bench *II* may support the floor lowering hypothesis: they are found in Capri Chasma and west Eos Chasma adjacent to ridged areas, and their morphology may suggest rotation and collapse of the bench margin in response to lowering of the neighboring floor. We note, however, that because wrinkle ridges on Mars are most commonly found in volcanic settings, it is possible that volcanic processes also formed the Valles Marineris ridges.

Finally, we observe another feature associated with the Coprates and Capri floor ridges, namely small cones, a few 100 m to 1 km in diameter, frequently (but not exclusively) with summit pits (Fig. 13d). Several candidate cone types exist, including cinder cones, tuff cones, rootless cones, pingos, and mud volcanoes. Mud volcanism may be a reasonable explanation in the context of a compressional environment (Komar, 1991), and similar cones have been attributed a mud volcano origin in Acidalia Planitia, north of the Chryse chaotic terrains (Farrand et al., 2005; Tanaka et al., 2003). However, once again, we note that a volcanic interpretation of these features (as cinder cones or tuff cones) is possible.

4. Discussion

Our first objective here is to present a possible history of lacustrine processes in the VMD region through the application of stratigraphic and morphological constraints. Our second objective is to address potential problems with the lacustrine interpretation: we consider the strength of alternative formation hypotheses and arguments concerning the mineralogy of the region.

4.1. History of lacustrine activity

4.1.1. Temporal constraints

Our hypothesis is that groundwater discharge at Capri and Eos chaotic terrains ponded in the VMD before being released into outflow channels and onward into the large northern plains basins. To first order then, we require groundwater discharge to postdate the formation of the central Valles Marineris (especially Coprates and Melas Chasmata). Chaotic terrains and the Valles Marineris canyons both formed in the late Hesperian (Tanaka, 1997; Lucchitta et al., 1992), but the presence of chaos and channels in tectonically generated depressions such as Echus and Juventae Chasmata suggest that the former features are younger. More detailed stratigraphic analyses also support this ordering (e.g., Chapman and Tanaka, 2002). A smooth channel deposit with streamlined features connects Eos and Aurorae Chasmata and constrains significant flooding from VMD overflow to be no younger than late Hesperian (Rotto and Tanaka, 1995).

Topographic considerations also constrain the timing of lacustrine activity. Capri Mensa, an interior deposit separating Capri and eastern Eos Chasmata, must have been in place prior to ponding. This is because the paleolake overflow point consists of channel features incised into the interior deposit: indeed, the deposit likely contributed significantly to the damming of groundwater discharge. Finally, the large channel and chaos structures downstream of Eos Chasma must have been in place prior to ponding. If Eos Chasma was closed at its eastern margin during ponding, water levels would not have been limited by the observed overflow point, and shoreline features would likely have formed along east Eos Chasma walls and massifs. Thus, the ponding of the VMD likely attended the late stages of groundwater discharge in Capri and Eos Chasmata. The appearance of benches at multiple elevations suggests that paleolake levels changed episodically, but remained at each elevation long enough for shorelines to develop. Such behavior is expected if groundwater discharge occurred episodically and produced varying quantities of water, a likely hydrological scenario (Harrison and Grimm, 2008;

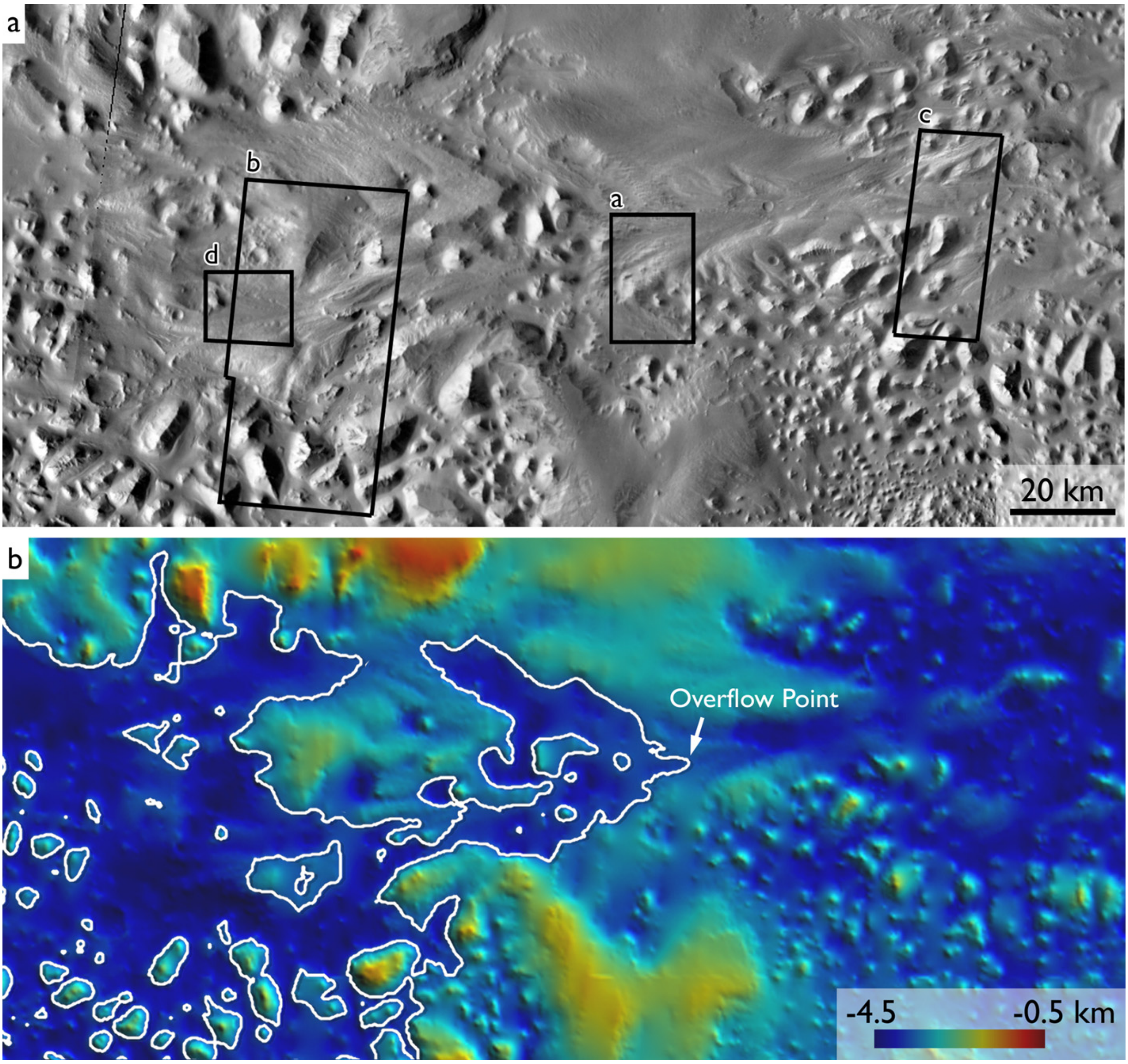

Fig. 11. Region where overflow from VMD is likely to have occurred. (a) THEMIS daytime IR mosaic and (b) shaded MOLA topography. White line indicates maximum ponding elevation contour. Overflow point ("OP") is associated with flow features, some of which are shown in greater detail in Fig. 12. Labeled boxes in (a) show position of Fig. 12 images.

Andrews-Hanna and Phillips, 2007). Those ponding episodes related to the lower, more pristine benches in Capri, eastern Coprates, and western Eos Chasmata, likely postdate the damming of the entire VMD, an event which produced the more degraded benches observed at higher elevations and as far west as Melas Chasma.

4.1.2. *Style of lacustrine processes*

Bench *I* appears to be composed of a series of wallrock-derived layers of variable strength (the layers were likely initially exposed by collapse of the Valles Marineris floor; Tanaka and Golombek, 1989). As suggested above, their common height close to the maximum ponding elevation of the VMD and their flat morphology relative to neighboring wallrock suggest that a hydrostatic agent contributed to erosion of weaker layers, enhancing terrace formation at the observed elevation. Wave action on Mars may have been relatively weak (Kraal et al., 2006), and erosion by ice-ridge pile up may be more likely (Barnhart et al., 2005). Identification of ridges of material pushed ashore by a moving ice-plug would support the latter process, while the former process may have been enhanced in the VMD by the long fetch of the inundated area, the likely high winds through the canyons, and water currents attending episodes of emptying and refilling of the VMD.

Bench *II* appears to be constructional, based largely on its pattern of broad, convex projections and narrow, sharp re-entrants (Howard, 1994, 1995; e.g., Fig. 9). Thus, we favor the process of bench formation invoked by Howard and Moore (2004) for the Gorgonum chaos benches that so closely resemble eastern VMD benches, namely the compression of sediments by an overlying floating ice cover. In this scenario, sediments may be deposited

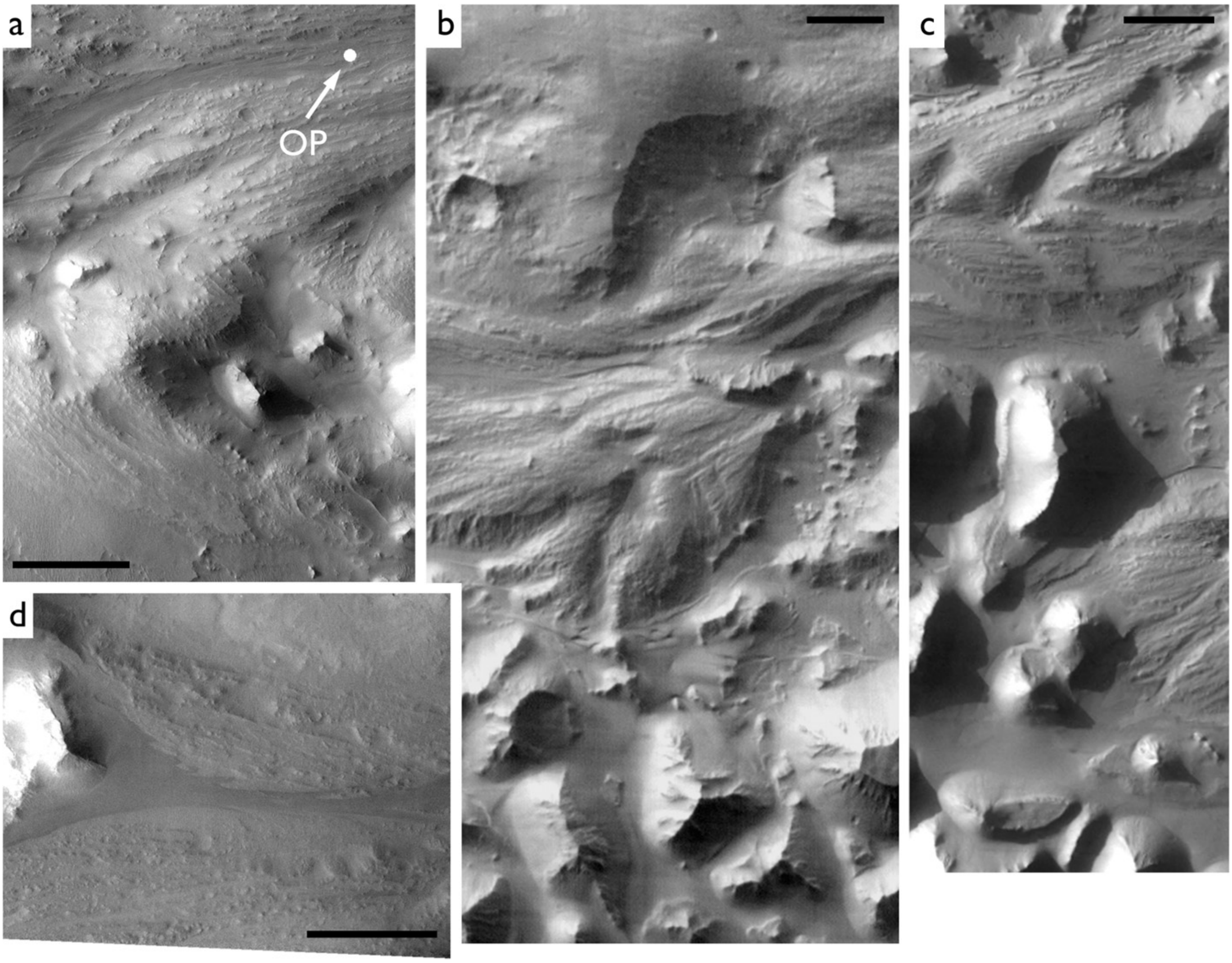

Fig. 12. Flow features in the vicinity of the MCCE overflow point. (a) Scour marks in the immediate neighborhood of the overflow point ("OP"). (b) Fluvial erosion upstream of the overflow point. (c) Similar features downstream of the overflow point, including braided channels (bottom right). (d) Flow toward the overflow point (to right of image, not shown) appears to have been parted by an obstacle (far left). Scale bars in all images correspond to 5 km. Image contexts are shown in Fig. 11. ((a) THEMIS VIS V18587004, (b) THEMIS daytime IR I04359002, (c) VIS V03535003, (d) VIS V17389003.)

originally through fluvial, lacustrine, or airfall processes. In the case of the Valles Marineris, an important contributor is likely to be mass wasting in the form of landsliding and talus accumulation. Indeed, the lobate form of some benches suggests initial emplacement by landsliding followed by significant deformation or degradation.

An alternative formation process for bench *II* is the dessication of a volatile-rich layer and associated floor collapse. Although bench *II* appears to be constructional, collapse is compatible with marginal bench fractures and nearby reticulated wrinkle ridge patterns. However, there is no direct evidence of past volatile content or transport in the floor deposit, and volcanic processes occurring some time after the last water ponding event may well explain the floor morphology (similarly to Hydraotes Chaos; Meresse et al., 2008). Certainly the volatile loss hypothesis is unlikely for the higher elevation bench *I* morphology, since an initial sediment layer on the order of 10 km thick (deeper than the current VM topography) is required, assuming typical porosity estimates of about 0.1. The alternative of a nearly pure ice layer 1.5 km thick buried below a significant layer of sediment (which would later become the collapsed canyon floor) also seems improbable: such thick ice layers are more likely to have formed on the surface due to precipitation at high obliquities (Mischna et al., 2003; Harrison and Grimm, 2004; Russell and Head, 2007).

Finally, we note that the lateral distribution of VMD benches is skewed toward the east, an observation that may be explained by the maximum ponding level of the region. One of the shallowest points of a putative lake filled to this level is approximately halfway along Coprates Chasma (at approximately 301° E; Figs. 1 and 2). Depths here range from 100 to 200 m, compared to a maximum lake depth (excluding crater floors) of about 1650 m. If lake water was provided predominantly by groundwater discharge at Capri and Eos chaotic terrains, ponding would have extended westward to Melas Chasma and western Coprates Chasma only if water levels came within 200 m of the maximum ponding elevation. However, the obstruction that imposes this constraint (which appears to be a landslide deposit spanning the width of the canyon) is estimated to be no more than a few 100 Myr old (Quantin et al., 2004), suggesting emplacement some time after lacustrine activity. If the landslide accounts for most of the topographic rise, it cannot have caused the skewed distribution of bench features, but if the pre-landslide surface was higher than the surrounding canyon floor, then it may have limited lacustrine activity to the west.

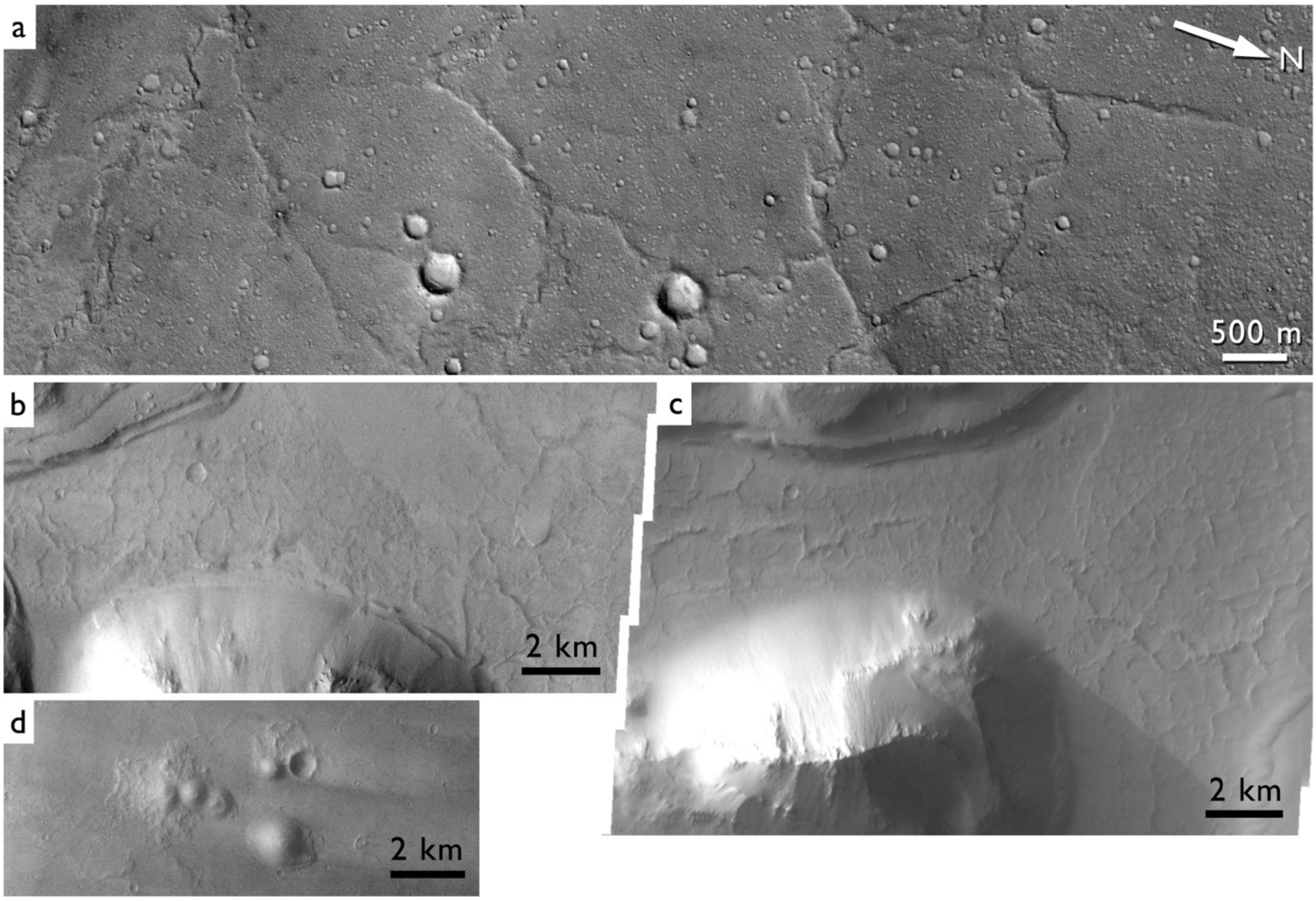

Fig. 13. Polygonally arranged ridges on Coprates and Capri Chasmata floors. Note the association of ridges in (b) and (c) with marginal fractures in benches at the top of each image. In (d), ridges are associated with cones. ((a) MOC NA e0200985, (b) THEMIS VIS V18113004, (c) V19648002, (d) V18625001.)

4.1.3. Alternative water source

The present day maximum ponding elevation of the VMD corresponds roughly to the -3760 ± 560 m elevation of the Contact 2 northern plains shoreline (Clifford and Parker, 2001), suggesting that the Valles Marineris paleolake might once have been part of a much larger northern ocean. This hypothesis is also supported by the similarity of bench *II* morphology with proposed wavecut terraces in the northern plains (Parker et al., 1993). Although water levels would initially need to exceed -3560 m in order to flood Melas and Coprates Chasma, this value is well within the error of the northern ocean shoreline elevation. As ocean levels later fell, water would have been trapped within the VMD, with breakout eventually occurring at the observed overflow point. The drawback of this hypothesis is the lack (thus far) of evidence supporting initial flow of water into, rather than out of, the Valles Marineris, and its inundation of other canyons exposed to the northern plains (such as Ganges Chasma and Hydaspis Chaos).

4.2. Non-lacustrine formation hypotheses

4.2.1. Faulting

The formation of the Valles Marineris involved substantial contributions from tectonic processes (for an overview, see Lucchitta et al., 1992). The possibility thus exists that the VMD benches are derived from motion along normal faults. Collapse related to tension fracturing may provide a plausible origin for bench *I* (Tanaka and Golombek, 1989). However, in many cases bench *I* (and more frequently bench *II*) margins are not linear as expected for fault scarps, but are arcuate, sometimes completely ringing massifs. Second, the orientation of many benches bears no spatial relationship to visible fault boundaries such as the linear Coprates Chasma walls (those benches that do appear along linear canyon walls cannot unambiguously be attributed a tectonic origin). Finally, the approximately uniform elevation of the benches (in contrast to their significantly undulating regional context) is not easily explained by a tectonic collapse origin.

4.2.2. Backwasting of resistant beds

As suggested above, the VMD bench *I* appears to be composed of backwasted resistant cliffs cropping out from the lowest level of the plateau wallrock. However, their flat morphology relative to neighboring wallrock, and their height approximately matching that of the maximum ponding level of the VMD leads us to suggest that they enclosed a putative paleolake that enhanced the erosional face of the cliffs. Beach *II* appears to be a constructional landform by virtue of its soft sinuous edge and narrow re-entrants, making a backwasting origin unlikely. Additionally, deposits of removed material in the form of talus cones and landslides are absent from the floors immediately in front of the bench *II* margin. Fluvial features are also absent from bench *II* scarps, although some are present on the relatively flat upper surfaces of bench *I* as described above: these features, however, indicate removal of material from the canyon wall behind the bench, rather than from the bench itself.

4.3. Mineralogy

Possible evidence against ponding in the VMD lies in the apparent dearth of mineralogic support. Thus far, almost no evidence of water-related minerals such as sulfates and phyllosilicates has been found within the maximum ponding level (Bibring et al., 2006; Mangold et al., 2007a). Also, olivine (which is unstable in aqueous conditions) is found in high concentrations in basaltic outcroppings in some Chryse Planitia channels, although not within the VMD (Christensen et al., 2003; Edwards et al., 2007).

The absence of phyllosilicates is not unexpected. These minerals are thought to have formed predominantly in the Noachian (the "phyllosian") before outflow channel formation and the proposed surface ponding (Bibring et al., 2006). Although Noachian layering is exposed in the Valles Marineris walls, the presence (or lack) of phyllosilicates in these layers is likely a consequence of their Noachian origin prior to canyon formation. If, instead, phyllosilicate formation was still occurring in parts of the planet during VMD ponding, the absence of these minerals in the VMD, together with their requirement of a long-term source of water (Mangold et al., 2007b) may limit VMD ponding to short periods of time, in agreement with the episodic nature of lake formation and failure described above.

Sulfates, on the other hand, are present in parts of the Valles Marineris but are closely associated with freshly exhumed scarps in interior layered deposits. Their absence from gently sloping and dust-mantled paleolake floors in the VMD thus seems reasonable. Ultimately though, alternative processes such as groundwater alteration or ice–magma interactions may explain both the sulfates and their correlation with interior layered deposits (Gendrin et al., 2005; Chapman and Tanaka, 2002). In this case, the lack of sulfate production during subsequent lake formation may be the result of unfavorable mineralogic and thermal conditions.

Finally, olivine-rich basalts in Chryse Planitia appear to conflict with the occurrence of surface flooding: outcrops occur in channel banks and occasionally on channel floors. Perhaps transient floods are not sufficiently long-lived to produce the weathering necessary to destabilize olivine. Furthermore, terrestrial flows lasting significant periods have been observed to leave olivine basalts unaltered (e.g., Grand Canyon olivine basalts at Lava Falls; Hamblin, 1994). Nonetheless, no olivine-rich outcrops have yet been identified in circum-Chryse chaotic terrain depressions that likely held standing bodies of water (Edwards et al., 2007).

5. Conclusions

Observation of numerous bench structures along the walls of Melas, Coprates, Capri and Eos Chasmata suggest the past presence of a standing body of water, part of which was released, perhaps episodically, into outflow channels and thence into the northern plains. Coincidence of the MOLA-derived basin overflow point with the only occurrence of channel erosion in the region strongly supports the ponding hypothesis. If the maximum water levels are assumed to be limited by the present day maximum ponding level, and if the elevation of the canyon floor has not changed significantly since the early Hesperian, then the average depth of the paleolake is estimated to be 840 m, with a total volume of 110,000 km^3. Although the most likely source of ponded water was groundwater discharge at chaotic terrain in Capri and Eos Chasmata, an alternative supply from a northern plains ocean, which has a putative shoreline at a similar elevation to the Valles Marineris paleolake, is possible.

Acknowledgments

This work was supported by NASA Grant NNG05GL83G. Thanks to Sebastian Breitenbach, Wendy Jaegar, Bob Grimm, Ginny Gulick, and Ken Tanaka for valuable input. We also wish to thank the HRSC Team and Gerhard Neukum for some of the topographic profiles.

References

Andrews-Hanna, J.C., Phillips, R.J., 2007. Hydrological modeling of outflow channels and chaos regions on Mars. J. Geophys. Res. 112, doi:10.1029/2006JE002881.

Barnhart, C.J., Tulaczyk, S., Asphaug, E., Kraal, E.R., Moore, J., 2005. Ice-ridge pile up and the genesis of martian "shorelines". Lunar Planet. Sci. 36. Abstract 1560.

Bibring, J.-P., Langevin, Y., Mustard, J.F., Poulet, F., Arvidson, R., Gendrin, A., Gondet, B., Mangold, N., Pinet, P., Forget, F., the OMEGA Team, 2006. Global mineralogical and aqueous Mars history derived from OMEGA/Mars Express data. Science 312, 400–404.

Bretz, J.H., Smith, H.T.U., Neff, G.E., 1956. Channeled scabland of Washington—New data and interpretations. Geol. Soc. Am. Bull. 67, 957–1049.

Carr, M.H., 1974. Tectonism and volcanism of the Tharsis region of Mars. J. Geophys. Res. 79, 3943–3949.

Carr, M.H., 1996. Water on Mars. Oxford University Press, New York.

Chapman, M.G., Scott, D.H., 1989. Geology and hydrology of the north Kasei Valles area, Mars. Proc. Lunar Sci. Conf. 19, 367–375.

Chapman, M.G., Tanaka, K.L., 2002. Related magma–ice interactions: Possible origins of chasmata, chaos, and surface materials in Xanthe, Margaritifer, and Meridiani Terrae, Mars. Icarus 155, 324–339.

Christensen, P.R., and 21 colleagues, 2003. Morphology and composition of the surface of Mars: Mars Odyssey THEMIS results. Science 300, 2056–2061.

Clifford, S.M., Parker, T.J., 2001. The evolution of the martian hydrosphere: Implications for the fate of a primordial ocean and the current state of the northern plains. Icarus 154, 40–79.

Coleman, N.M., Baker, V., 2007. Evidence that a paleolake overflowed the rim of Juventae Chasma, Mars. Lunar Planet. Sci. 38. Abstract 1046.

Coleman, N.M., Dinwiddie, C.L., Baker, V.R., 2007. Evidence that floodwaters filled and overflowed Capri Chasma, Mars. Geophys. Res. Lett. 34, doi:10.1029/2006GL028872.

Di Achille, G., Ori, G.G., Reiss, D., 2007. Evidence for late Hesperian lacustrine activity in Shalbatana Vallis, Mars. J. Geophys. Res. 112, doi:10.1029/2006JE002858.

Edwards, C.S., Christensen, P.R., Hamilton, V.E., 2007. Evidence for extensive olivine-rich basalt bedrock outcrops in Ganges and Eos Chasma on Mars. In: 7th Int. Conf. Mars. Abstract 3280.

Farrand, W.H., Gaddis, L.R., Keszthelyi, L., 2005. Pitted cones and domes on Mars: Observations in Acidalia Planitia and Cydonia Mensae using MOC, THEMIS, and TES data. J. Geophys. Res. 110, doi:10.1029/2004JE002297.

Gendrin, A., Mangold, N., Bibring, J.-P., Langevin, Y., Gondet, B., Poulet, F., Bonello, G., Quantin, C., Mustard, J., Arvidson, R., LeMouélic, S., 2005. Sulfates in martian layered terrains: The OMEGA/Mars Express view. Science 307, 1587–1591.

Glotch, T.D., Christensen, P.R., 2005. Geologic and mineralogic mapping of Aram Chaos: Evidence for a water-rich history. J. Geophys. Res. 110, doi:10.1029/2004JE002389.

Greeley, R., Kuzmin, R.O., Nelson, D.M., Farmer, J.D., 2003. Eos Chasma, Mars: Regional setting for a potential landing site for astrobiology. J. Geophys. Res. 108, doi:10.1029/2002JE002014.

Hamblin, K.W., 1994, Late Cenozoic lava dams in the western Grand Canyon. GSA Memoir, vol. 183, 139 pp.

Harrison, K.P., Grimm, R.E., 2004. Tharsis recharge: A source of groundwater for martian outflow channels. Geophys. Res. Lett. 31, doi:10.1029/2004GL020502.

Harrison, K.P., Grimm, R.E., 2005. Groundwater-controlled valley networks and the decline of surface runoff on early Mars. J. Geophys. Res. 110, doi:10.1029/2005JE002455.

Harrison, K.P., Grimm, R.E., 2008. Multiple flooding events in martian outflow channels. J. Geophys. Res. 113, doi:10.1029/2007JE002951.

Hartmann, W.K., 1973. Martian surface and crust: Review and synthesis. Icarus 19, 550–575.

Howard, A.D., 1994. Rockslopes. In: Abrahams, A.D., Parsons, A.J. (Eds.), Geomorphology of Desert Environments. Chapman & Hall, London, pp. 123–172.

Howard, A.D., 1995. Simulation modeling and statistical classification of escarpment planforms. Geomorphology 12, 187–214.

Howard, A.D., Moore, J.M., 2004. Scarp-bounded benches in Gorgonum Chaos, Mars: Formed beneath an in ice-covered lake? Geophys. Res. Lett. 31, doi:10.1029/2003GL018925.

Irwin, R.P., Maxwell, T.A., Howard, A.D., Craddock, R.A., Leverington, D.W., 2002. A large paleolake basin at the head of Ma'adim Vallis, Mars. Science 296, 2209–2212. 5576.

Komar, P.D., 1991. Mud volcanoes on Mars? Reports Plan. Geol. Geophys. Prog. N92-10728 01-91, pp. 539–541.

Komatsu, G., Geissler, P.E., Strom, R.G., Singer, R.B., 1993. Stratigraphy and erosional landforms of layered deposits in Valles Marineris, Mars. J. Geophys. Res. 98, 11105–11121.

Komatsu, G., Kargel, J.S., Baker, V.R., Strom, V.R., Ori, G.G., Mosangini, C., Tanaka, K.L., 2000. A chaotic terrain hypothesis: Explosive outgas and outflow by dissociation of clathrate on Mars. Lunar Planet. Sci. 31. Abstract 1434.

Kraal, E.R., Asphaug, E., Moore, J.M., Lorenz, R.D., 2006. Quantitative geomorphic modeling of martian bedrock shorelines. J. Geophys. Res. 111, doi:10.1029/2005JE002567.

Lucchitta, B.K., 1979. Landslides in Valles Marineris, Mars. J. Geophys. Res. 84, 8097–8113.

Lucchitta, B.K., McEwen, A.S., Clow, G.D., Geissler, P.E., Singer, R.B., Schultz, R.A., Squyres, S.W., 1992. The canyon system on Mars. In: Keiffer, H.H., Jakosky, B.M., Snyder, C.W., Matthews, M.S. (Eds.), Mars. Univ. of Arizona Press, Tucson, pp. 453–492.

Lucchitta, B.K., Isbell, N.K., Howington-Kraus, A., 1994. Topography of Valles Marineris: Implications for erosional and structural history. J. Geophys. Res. 99 (2), 3783–3798.

Mangold, N., Quantin, C., Ansan, V., Delacourt, C., Allemand, P., 2004. Evidence for precipitation on Mars from dendritic valleys in the Valles Marineris area. Science 305, 78–81.

Mangold, N., Gendrin, A., Quantin, C., Bibring, J.-P., Gondet, B., Langevin, Y., Poulet, F., Arvidson, R., Griffes, J.L., Hauber, H., Masson, P., Neukum, G., the OMEGA Team, HRSC Co-Investigator Teams, 2007a. An overview of the sulfates detected in the equatorial regions by the OMEGA/MEX spectrometer. In: 7th Int. Mars Conf. Abstract 3141.

Mangold, N., Poulet, F., Mustard, J.F., Bibring, J.P., Gondet, B., Langevin, Y., Ansan, V., Masson, P., Fassett, C., Head III, J.W., Hoffman, H., Neukum, G., 2007b. Mineralogy of the Nili Fossae region with OMEGA/Mars Express data. 2. Aqueous alteration of the crust. J. Geophys. Res. 112, doi:10.1029/2006JE002835.

Masursky, H., Boyce, J.M., Dial Jr., A.L., Schaber, G.G., Strobell, M.E., 1977. Classification and time of formation of martian channels based on Viking data. J. Geophys. Res. 8, 4016–4038.

Max, M.D., Clifford, S.M., 2000. The initiation of martian outflow channels through the catastrophic decomposition of methane hydrate. Lunar Planet. Sci. 31. Abstract 2094.

Mège, D., Cook, A.C., Garel, E., Lagabrielle, Y., Cormier, M.-H., 2003. Volcanic rifting at martian grabens. J. Geophys. Res. 108, doi:10.1029/2002JE001852.

Meresse, S., Costard, F., Mangold, N., Masson, P., Neukum, G., the HRSC Co-I Team, 2008. Formation and evolution of the chaotic terrains by subsidence and magmatism: Hydraotes Chaos, Mars. Icarus 194, 487–500.

Mischna, M.A., Richardson, M.I., Wilson, R.J., McCleese, D.J., 2003. On the orbital forcing of martian water and CO_2 cycles: A general circulation model study with simplified volatile schemes. J. Geophys. Res. 108, E6, doi:10.1029/2003JE002051.

Ori, G.G., Mosangini, C., 1998. Complex depositional systems in Hydraotes Chaos, Mars: An example of sedimentary process interactions in the martian hydrologic cycle. J. Geophys. Res. 103, 22713–22723.

Parker, T.J., Gorsline, D.S., Saunders, R.S., Pieri, D.C., Schneeberger, D.M., 1993. Coastal geomorphology of the martian northern plains. J. Geophys. Res. 98, 11061–11078.

Perron, J.T., Mitrovica, J.X., Manga, M., Matsuyama, I., Richards, M.A., 2007. Evidence for an ancient martian ocean in the topography of deformed shorelines. Nature 447, 840–843.

Peulvast, J., Mège, D., Chiciak, J., Costard, F., Masson, P.L., 2001. Morphology, evolution and tectonics of Valles Marineris wallslopes (Mars). Geomorphology 37, 329–352.

Quantin, C., Allemand, P., Mangold, N., Delacourt, C., 2004. Ages of Valles Marineris (Mars) landslide and implications for canyon history. Icarus 172, 555–572.

Rotto, S., Tanaka, K.L., 1995. Geologic/geomorphic map of the Chryse Planitia region of Mars. US Geol. Surv. Misc. Invest. Ser. Map I-2441, scale 1:5,000,000.

Russell, P.S., Head, J.W., 2007. The Martian hydrologic system: Multiple recharge centers at large volcanic provinces and the contribution of snowmelt to outflow channel activity. Planet. Space Sci. 55, 315–332.

Saunders, R.S., 1979. Geologic map of the Margaritifer Sinus quadrangle of Mars. US Geol. Surv. Misc. Invest. Ser. Map I-1144, scale 1:5,000,000.

Schultz, R.A., 1991. Structural development of Coprates Chasma and western Ophir Planum, Valles Marineris Rift, Mars. J. Geophys. Res. 96, 22777–22792.

Scott, D.H., Tanaka, K.L., 1986. Geologic map of the western equatorial region of Mars. US Geol. Surv. Misc. Invest. Ser. Map I-1802-A, scale 1:15,000,000.

Sharp, R.P., 1973. Mars–Troughed terrain. J. Geophys. Res. 78 (20), 4063–4072.

Smith, D.E., and 18 colleagues, 1999. The global topography of Mars and implications for surface evolution. Science 284, 1495–1503.

Tanaka, K.L., 1997. Sedimentary history and mass flow structures of Chryse and Acidalia Planitiae, Mars. J. Geophys. Res. 102, 4131–4149.

Tanaka, K.L., Golombek, M.P., 1989. Martian tension fractures and the formation of grabens and collapse features at Valles Marineris. Proc. Lunar Sci. Conf. 19, 383–396.

Tanaka, K.L., Skinner, J.A., Hare, T.M., Joyal, T., Wenker, A., 2003. Resurfacing history of the northern plains of Mars based on geologic mapping of Mars Global Surveyor data. J. Geophys. Res. 108 (E4), doi:10.1029/2002JE001908.

Wise, D.U., Golombek, M.P., McGill, G.E., 1979. Tharsis province of Mars: Geologic sequence, geometry, and a deformation mechanism. Icarus 38, 456–472.

Witbeck, N.E., Tanaka, K.L., Scott, D.H., 1991. The geologic map of the Valles Marineris region, Mars. US Geol. Surv. Misc. Invest. Ser. Map I-2010, scale 1:2,000,000.